Blistering of supported lipid membranes induced by Phospholipase D, as observed by real-time atomic force microscopy

Karim El Kirat [*,1], Vincent Duprès, Yves F. Dufrêne

Unité de chimie des interfaces, Université catholique de Louvain, Croix du Sud 2/18, B-1348 Louvain-la-Neuve, Belgium

Abstract

Phospholipase D from *Streptomyces chromofuscus* (PLDSc) is a soluble enzyme known to be activated by the phosphatidic acid (PA)–calcium complexes. Despite the vast body of literature that has accumulated on this enzyme, the exact mechanism of activation remains poorly understood. In this work, we report the first observation of PLDSc activity in real time and at nanometer resolution using atomic force microscopy (AFM). AFM images of continuous and patchy dipalmitoylphosphatidylcholine (DPPC) bilayers were recorded, prior and after incubation with PLDSc. For continuous bilayers, the enzyme induced important morphological alterations; holes corresponding to the bilayer thickness were created, while an additional elevated phase, about 2.5 nm high, was observed. This bilayer blistering is believed to be due to the production of the negatively charged lipid PA that would cause localized repulsions between the bilayer and the underlying mica surface. By contrast, these elevated domains were not seen on patchy bilayers incubated with the enzyme. Instead, the shapes of DPPC patches were strongly deformed by enzyme activity and evolved into melted morphologies. These results point to the importance of lipid packing on PLD activity and illustrate the potential of AFM for visualizing remodeling enzymatic activities.
© 2007 Elsevier B.V. All rights reserved.

Keywords: Atomic force microscopy; Lipid bilayers; Phospholipase D; Phosphatidic acid; Membrane blistering; Anionic lipid

1. Introduction

Phospholipase D (PLD) catalyzes the hydrolysis of the phosphodiester bond between the phosphatidyl-moiety and the choline headgroup of phosphatidylcholine (PC) which liberates phosphatidic acid (PA) and free choline. The hydrolytic activity catalyzed by PLD occurs with P–O bond cleavage of PC as demonstrated previously [1]. The PLD from *Streptomyces chromofuscus* (PLDSc) belongs to the PLD superfamily as well as some endonucleases, helicases, lipid synthases and many other enzymes catalyzing the hydrolysis and/or the formation of phosphodiester bonds [2]. However, PLDSc is unique among these proteins as its enzymatic activity is calcium dependent

[3,4] and it does not possess the classical HKD catalytic site [5]. Furthermore, this bacterial PLD is activated by anionic lipids, for which it also exhibits a high affinity [4–7]. Indeed, PA is thought to be an allosteric activator of PLDSc [8], but the nature of this activation has never been clearly identified. Moreover, Brewster angle microscopy also shows that PLDSc forms large aggregates under PA monolayers [7].

Several protocols have been developed for the measurement of PLD activity [9]. The most common methods are based on radioactive assays, pH-stat, [1H] nuclear magnetic resonance [8], and choline oxidase electrodes [3]. New approaches were proposed recently especially with lipid monolayers and the Langmuir film technique [4,7], and polarization modulation infrared reflection-absorption spectroscopy at the air–water interface [10]. Soluble substrates of PLD were employed as well to define the influence of membrane structure on enzyme activity [4,11,12]. All these studies concluded that PLD is activated by both PA and calcium. However, direct in situ observation of the PLD activity on lipid membranes has never been reported.

* Corresponding author. Tel./fax: +33 344237943.
 E-mail address: kelkirat@utc.fr (K. El Kirat).
[1] Present address: UMR CNRS 6600, Biomécanique et Génie Biomédical, Université de Technologie de Compiègne, BP 20529, 60205 Compiègne Cedex, France.

Atomic force microscopy (AFM) is a valuable tool for imaging lipid bilayers [13–16] and to explore their interaction with external agents such as detergents [17–21], solvents/buffers [22,23], peptides [24–26], and proteins [27]. Phospholipases are able to catalyze the hydrolysis of phospholipids yielding lipids with new characteristics. In this context, AFM has been used to visualize alterations induced in lipid bilayer by the enzyme phospholipase A2 (PLA2) which catalyzes hydrolysis of the ester linkage (in sn-2 position) of glycerophospholipids to produce fatty acid and lyso-phospholipid. In a pioneering study, Grandbois et al. [28] investigated the degradation of gel DPPC bilayers by PLA2 by recording a sequence of images at different stages of enzyme reaction. This study evidenced that defects in the membrane enhanced PLA2 activity. AFM experiments also permitted to visualize the so-called lag-burst kinetics of PLA2, a kinetic phenomenon in which the rate of hydrolysis suddenly changes from a regime of low activity to a regime of high hydrolysis rate [29]. In a study on the effect of PLA2 on two-component bilayers, Kaasgaard et al. [30] showed the preference of PLA2 for dimyristoylphosphatidylcholine phases compared to distearoylphosphatidylcholine phases. An AFM study on PLA2 also reported on the application of lipases in nanolithography of lipid membranes [31]. More recently, an AFM tip modified with PLD was used
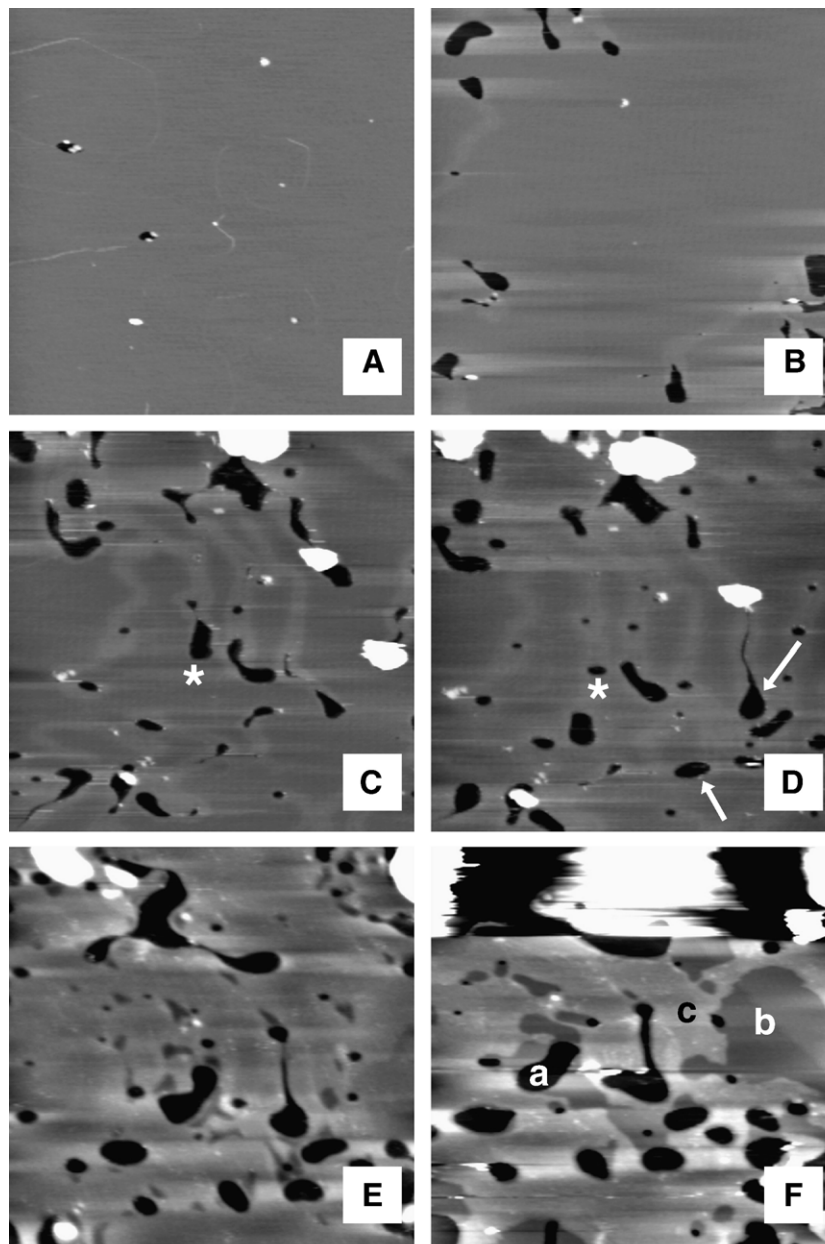

Fig. 1. PLDSc-catalyzed digestion of supported lipid bilayers. A DPPC bilayer was imaged with AFM under Tris/calcium buffer (A, 8×8 μm^2, $z = 10$ nm). PLDSc (10 μg/mL) was then added to the medium in the same buffer and the reaction was monitored at different incubation times: (B) 4, (C) 7, (D) 15, (E) 40 and (F) 55 min. Asterisk in panel C indicates a fixed point where a hole is about to resorb as compared to panel D. Arrows in panel D correspond to newly formed holes. In F, marks correspond to: a, the underlying mica; b, the DPPC surface; and c, the newly formed elevated phase corresponding to membrane blistering.

to generate PA in very localized areas of a supported PC bilayer [32].

Here, we used AFM to visualize in real time the effect of PLDSc on the organization of supported dipalmitoylphosphatidylcholine (DPPC) bilayers. Time lapse images demonstrated that PLDSc activity induces the formation of elevated phases attributed to the accumulation of negatively charged PA lipids. This original AFM study of the PLD activity provides new insight into the mechanism of action of this enzyme.

2. Materials and methods

2.1. Materials

L-α-dipalmitoylphosphatidylcholine (DPPC) and Phospholipase D from S. chromofuscus (PLDSc) were purchased from Sigma (St. Louis, MO) and used without further purification. The SDS-PAGE analysis of PLD gave the same three bands as those obtained by Geng et al. [33]. These proteins have been previously identified by sequence analysis [33] as the intact PLD (57 kDa) and its two proteolytically processed fragments (20 kDa, and an active fragment of 42 kDa). PLDSc was solubilized at 10 μg/mL in Tris/calcium imaging buffer (10 mM Tris, 150 mM NaCl, 120 μM calcium, pH 8.0).

2.2. Preparation of supported lipid bilayers

Supported lipid bilayers were prepared using a two step vesicle fusion method [34,35]. To this end, DPPC was dissolved in chloroform at 0.6 mM final concentration. This organic solution was then evaporated under nitrogen and dried in a dessicator under vacuum for 2 h. Multilamellar vesicles (MLV) were obtained by resuspending the lipidic dried film in Tris/calcium buffer at 0.6 mM final lipid concentration. To obtain small unilamellar vesicles (SUV), the suspension was sonicated to clarity (4 cycles of 2 min) using a 500 W probe sonicator (Fisher Bioblock Scientific, France; 35% of the maximal power; 13 mm probe diameter) while keeping the suspension in an ice bath. The liposomal suspension was then filtered on 0.2 μm nylon filters (Whatman Inc., USA) to eliminate titanium particles. Freshly cleaved mica squares (16 mm^2) were glued onto steel sample discs (Veeco Metrology LLC, Santa Barbara, CA) using Epotek 377 (Gentec Benelux, Waterloo, Belgium). 150 μL of the SUV suspension were deposited onto the mica samples and the vesicles were allowed to adsorb to the mica for 10 h at 4 °C, as previously described [34,35]. Subsequently, samples were rinsed ten times with 150 μL of Tris/calcium imaging buffer (10 mM Tris, 150 mM NaCl, 120 μM calcium, pH 8.0) and then heated to 60 °C for 60 min. Samples were allowed to cool slowly to room temperature and then immediately analyzed by AFM. Most of the DPPC bilayers were continuous, but occasionally some DPPC membranes were rich in defects. The latter served to investigate the influence of defects on PLD activity.

2.3. Atomic force microscopy

Supported bilayers were investigated using a commercial AFM (NanoScope IV MultiMode AFM, Veeco Metrology LLC, Santa Barbara, CA) equipped with a 125 μm × 125 μm × 5 μm scanner (J-scanner) and a standard AFM liquid cell without the O-ring. Topographic 256 × 256 pixel images were recorded in contact mode using oxide-sharpened microfabricated Si$_3$N$_4$ triangular cantilevers (length 320 μm, Microlevers, Veeco Metrology LLC, Santa Barbara, CA) with spring constant of 0.01 N/m (manufacturer specified), with a minimal applied force (<500 pN) and at a scan rate of 5–6 Hz. Images were obtained at room temperature (23–25 °C) in Tris/calcium imaging buffer before and after the injection of PLDSc. The enzyme was added by replacing the Tris/calcium imaging buffer in the AFM liquid cell and on the sample with the Tris/calcium imaging buffer containing the PLDSc at 10 μg/mL. For real-time imaging, successive AFM images were recorded at increasing times, while retracting the tip from the bilayer surface between each image to minimize any potential sample alteration by the scanning tip.

3. Results and discussion

3.1. Continuous DPPC bilayers

Studying the interaction of phospholipase enzymes with lipid membranes at high resolution may be useful to understand their mode of action. To probe the hydrolytic activity of PLDSc in real time, continuous DPPC bilayers were prepared by vesicle fusion on mica and imaged by AFM in Tris/calcium imaging buffer either in the absence or in the presence of the enzyme. As shown in Fig. 1A, the topographic image obtained for a native DPPC bilayer revealed the presence of a continuous phase decorated with some holes and small particles. The holes' depth, 5.5 ± 0.1 nm, is roughly consistent with the DPPC bilayer thickness [24,25], while the particles may be attributed to unfused vesicles. To assess the stability of native DPPC bilayers during consecutive scans, successive images of the same bilayer location were recorded. Scanning the bilayer surface for 60 min did not cause any significant change of the surface morphology, indicating that the bilayer was stable in these conditions (data not shown).

The DPPC bilayers were then incubated with a 10 μg/mL PLDSc solution and successive images were recorded at the same location (Fig. 1B–F). After 4 min incubation (Fig. 1B), some large, round-shaped holes appeared, with a depth corresponding to the bilayer thickness (5.6 ± 0.2 nm). It is noteworthy that DPPA in the presence of calcium is able to form bilayers [36]. After 7 min (Fig. 1C), the morphology of the same region evolved slowly; some new holes appeared and became larger while others faded or even disappeared. These results provide
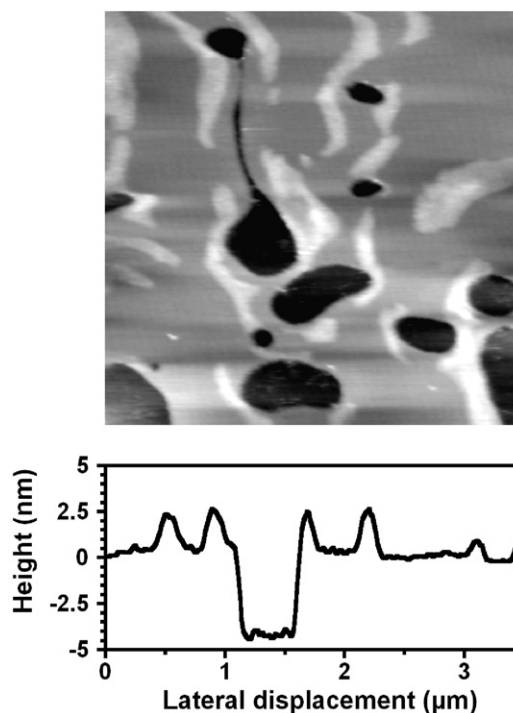

Fig. 2. High-resolution image of the PLDSc activity. Higher magnification of the same region as in Fig. 1 recorded 30 min after PLDSc injection (A, 3.5×3.5 μm^2, $z = 10$ nm) and the corresponding section taken along the white line.

direct evidence of the remodeling activity of PLDSc, as these enzymes are able to reorganize the membranes by forming and filling holes [37].

As one can see in Fig. 1D, after 15 min of incubation, some holes disappeared while new holes were formed. After 40 min (Fig. 1E), most holes grew in size while the morphology of the membrane was strongly modified in that an upper layer, 2.5 ± 0.2 nm thick, appeared and covered most of the bilayer surface. We suggest that this new protruding phase may correspond to the blistering of the bilayer as previously described for anionic lipids [38]. After 55 min (Fig. 1F), a three phase system was clearly observed: underlying mica (see mark a on Fig. 1F), supported DPPC bilayer (mark b on Fig. 1F) and an elevated phase of about 2.5 nm height (mark c on Fig. 1F). At longer contact times, the image contrast became very poor presumably due to bilayer detachment from the surface (data not shown). It is worth noting that other concentrations of PLDSc were also tested but the results did not permit to quantify the enzyme activity (data shown). Indeed, three kinds of morphological changes were simultaneously observed (holes forming/filling and blistering).

Fig. 2 shows the bilayer surface at higher magnification acquired 35 min after PLDSc addition. The underlying mica, the supported DPPC bilayer and the 2.5 nm elevated phase can clearly be distinguished. We suggest that these elevated domains, which were always well delimited and presented a

homogeneous height, correspond to an increased spacing between the bilayer and the underlying mica. These localized blisterings of the membrane may be provoked by the repulsive forces between the negatively charged DPPA and the underlying mica, as reported in a previous AFM study of membranes containing anionic lipids [38]. Rinia et al. [38] showed that anionic lipids were able to migrate from the top leaflet of the bilayer to the leaflet in contact with the mica in initially asymmetric membranes prepared by the Langmuir–Blodgett transfer technique. To explain this exchange of lipids, the authors postulated that the bilayer may present a convex curvature at the edge of the defects thus connecting the two leaflets. It is also noteworthy that the PLD molecules were never visible at the surface of the membrane.

3.2. Discontinuous DPPC bilayers

It is believed that the activity of phospholipases in membranes is modulated by the molecular organization of the lipid bilayer [28]. In particular, defects in gel-phase bilayers have been suggested to promote and act as starting points for the enzyme activity [28,31] and for protein insertion [27]. To address the question as to whether the PLDSc activity is enhanced by the presence of defects, discontinuous DPPC bilayers were incubated in the presence of the enzyme. Fig. 3A reveals a heterogeneous patchy DPPC bilayer covering $55 \pm 1\%$ of the
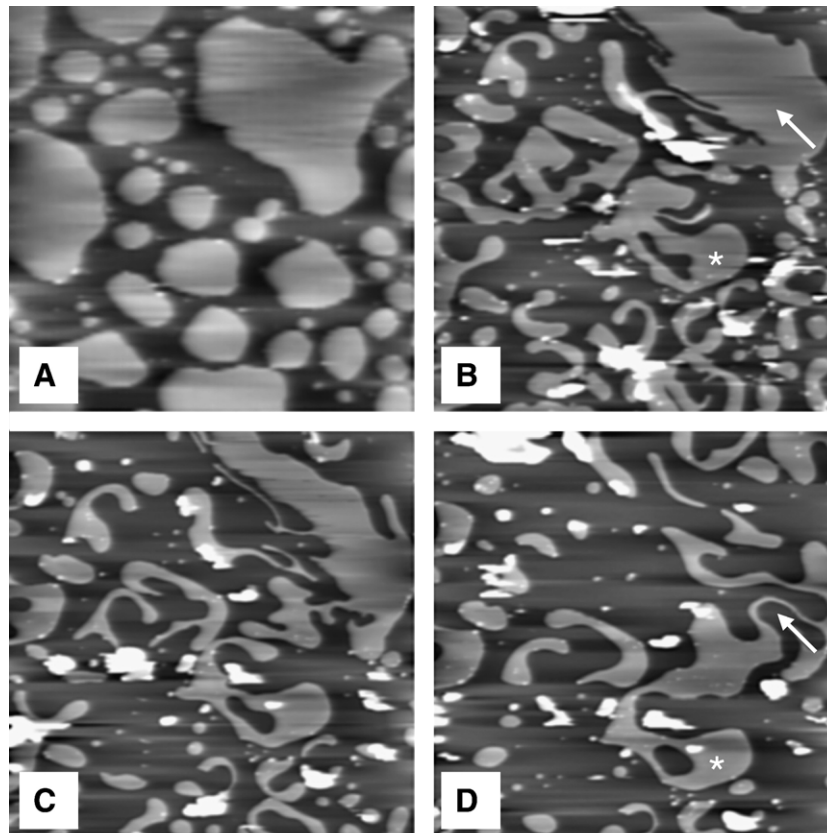

Fig. 3. PLDSc-catalyzed digestion of patchy bilayers. DPPC patches were imaged with AFM under Tris/calcium buffer (A, 10×10 μm², $z = 10$ nm). PLDSc (10 mg/mL) was then added to the medium in the same buffer and the reaction was monitored as follows: (B) 5, (C) 10, (D) 30 min. The white asterisk in panel B serves for the identification of a slowly evolving domain (see panel D). The white arrow points out a fast modification area of the DPPC patches.
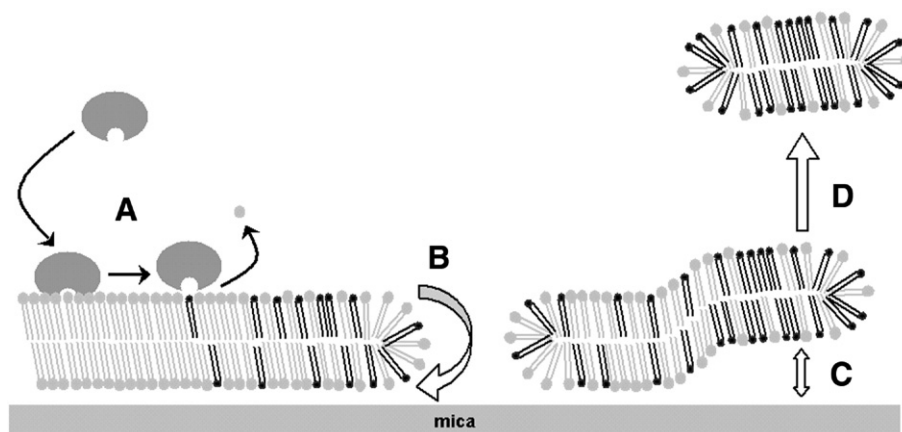
Fig. 4. Schematic representation of PLDSc-induced bilayer blistering as visualized by AFM. In step A, PLDSc catalyzes the hydrolysis of a DPPC molecule (depicted as grey lipid molecule) to yield PA (black lipid molecules) and free choline. As they concentrate in the upper leaflet accessible to PLD activity, molecules of DPPA could then reach the lower leaflet by passive diffusion via connecting convex edges of membrane defects (step B). As a consequence of DPPA accumulation in the lower leaflet, the blistering of the membrane would result from the moderate detachment induced by repulsive forces with the negative underlying mica surface (step C). Detachment at the edge of large defects would cause a massive desorption of bilayer parts, leading to the decrease of the total area covered by the membrane (step D).

scanned area. Bilayer patches could be imaged repeatedly without affecting their morphology. By contrast, after addition of PLDSc, the sample organization changed dramatically, even at short incubation times (Fig. 3B–D). After 5 min (Fig. 3B), patches were partially eroded, yielding a surface coverage of 46± 1%, and they showed complex, elongated shapes reminiscent of a melting material. This elongation may be related to the remodeling activity of PLDSc on membranes. Indeed, PLDs are often involved in membrane trafficking, budding and fusion events at the surface of living cells [39–41]. The observed alterations are much more pronounced than those observed after 7 min on homogeneous bilayers (Fig. 1B), suggesting that the enzyme activity was enhanced in defect-rich membranes. Indeed, in discontinuous DPPC membranes, the abundant defects constitute preferential sites for PLDSc activity due to the weaker packing of the lipids at the edge of the patchy DPPC bilayers as compared to a continuous bilayer. After 10 min (Fig. 3C), the patches represented 37±1% of the scanned surface. Furthermore, no blistering effect could be observed on the DPPC patches, suggesting that the bilayer digestion occurred essentially at the edges. The elongated shape of the digested patches may reflect the reorganization of the membrane due to a fast generation of DPPA. Since DPPA formation produced an increased spacing of the membrane with the underlying mica, and considering that the bilayer is enriched in defects surrounding the patches, we suppose that the DPPA rich edges may desorb progressively. Indeed, the repulsive interaction of DPPA enriched membrane edges with the mica may have led to their desorption. After 30 min (Fig. 3D), the surface coverage decreased again, to 28±1%. The large patch initially located in the upper right part of the image completely disappeared, while some patches became larger, apparently as a result of lateral merging of small patches.

The fact that patchy bilayers, thus large defects, promote the activity of lipases may be directly related to the enhanced accessibility of the enzymes in the interfacial region where molecular disorder is at maximum [28]. This would help the

enzymes to reach their substrates and to catalyze their hydrolysis. Again, PLDSc molecules were never found visible at the surface of the membrane and the mica.

3.3. Mechanism proposed for PLD induced blistering of membranes

Considering our results and the literature data, the following mechanism may be proposed to account for bilayer blistering induced by PLD (Fig. 4). First, PLDSc enzymes would reach the surface of the continuous bilayer and, in the presence of calcium, catalyze the conversion of DPPC into DPPA plus free choline (Fig. 4A). When enough DPPA molecules are generated, they would diffuse passively in the membrane and reach the lower leaflet through the connecting convex edges (Fig. 4B). Subsequently, the accumulation of the negatively charged DPPA lipids in the lower leaflet might promote the blistering of the membrane in some localized regions (Fig. 4C). When blisters occur along the boundary of sufficiently large defects, they may induce the desorption of large membrane parts (Fig. 4D).

As a consequence, at the end of PLDSc incubation, when all DPPC is converted into DPPA, the bilayer might float on the mica at a higher distance than that observed with PC lipids alone. This detachment may weaken the membrane, making it difficult to be scanned by the AFM tip without causing damages.

4. Conclusion

In this work, AFM was used to directly observe the influence of PLDSc on the nanoscale organization of supported DPPC bilayers, thereby providing new insight into its hydrolytic activity. Interestingly, after 40 min, a 2.5 nm thickening of the bilayer was observed, reflecting the blistering of the membrane by charge repulsion between DPPA and the mica. By contrast, for patchy bilayers we found that reorganization was much more pronounced than for continuous bilayers, while the elevated

phase was never observed, suggesting that digestion essentially occurred at the edge of the patches. Real-time AFM imaging of membrane digestion by PLDSc allowed the first direct visualization of membrane blistering phenomenon induced by anionic lipids accumulation. In the future, it would be interesting to quantify PLDSc reorganization activity on the basis of AFM imaging.

Acknowledgements

References

[1] P.G. Holbrook, L.K. Pannell, J.W. Daly, Phospholipase D-catalyzed hydrolysis of phosphatidylcholine occurs with P–O bond cleavage, Biochim. Biophys. Acta 1084 (1991) 155–158.

[2] C.P. Ponting, I.D. Kerr, A novel family of Phospholipase D homologues that includes phospholipid synthases and putative endonucleases: identification of duplicated repeats and potential active site residues, Protein Sci. 5 (1996) 914–922.

[3] I. Yamamoto, A. Konto, T. Handa, Regulation of Phospholipase D activity by neutral lipids in egg-yolk phosphatidylcholine small unilamellar vesicles and by calcium ion in aqueous medium, Biochim. Biophys. Acta 1233 (1995) 21–26.

[4] K. El Kirat, F. Besson, A.F. Prigent, J.P. Chauvet, B. Roux, Role of calcium and membrane organization on Phospholipase D localization and activity. Competition between a soluble and insoluble substrate, J. Biol. Chem. 277 (2002) 21231–21236.

[5] H. Yang, M.F. Roberts, Cloning, overexpression, and characterization of a bacterial Ca^{2+}-dependent Phospholipase D, Protein Sci. 11 (2002) 2958–2968.

[6] K. Stieglitz, B. Seaton, M.F. Roberts, The role of interfacial binding in the activation of *Streptomyces chromofuscus* Phospholipase D by phosphatidic acid, J. Biol. Chem. 274 (1999) 35367–35374.

[7] K. El Kirat, J.P. Chauvet, B. Roux, F. Besson, *Streptomyces chromofuscus* Phospholipase D interaction with lipidic activators at the air–water interface, Biochim. Biophys. Acta 1661 (2004) 144–153.

[8] D. Geng, J. Chura, M.F. Roberts, Activation of Phospholipase D by phosphatidic acid. Enhanced vesicle binding, phosphatidic acid-Ca^{2+} interaction, or an allosteric effect? J. Biol. Chem. 273 (1998) 12195–12202.

[9] A.J. Morris, M.A. Frohman, J. Engebrecht, Measurement of Phospholipase D activity, Anal. Biochem. 252 (1997) 1–9.

[10] I. Estrela-Lopis, G. Brezesinski, H. Mohwald, Dipalmitoyl-phosphatidylcholine/Phospholipase D interactions investigated with polarization-modulated infrared reflection absorption spectroscopy, Biophys. J. 80 (2001) 749–754.

[11] K.A. Stieglitz, B.A. Seaton, M.F. Roberts, Binding of proteolytically processed Phospholipase D from *Streptomyces chromofuscus* to phosphatidylcholine membranes facilitates vesicle aggregation and fusion, Biochemistry 40 (2001) 13954–13963.

[12] K. El Kirat, L. Volpon, B. Roux, F. Besson, Inhibition of *Streptomyces chromofuscus* Phospholipase D by antifungal lipopeptides from *Bacillus subtilis*, J. Antibiot. 57 (2004) 535–536.

[13] M.-C. Giocondi, V. Vié, E. Lesniewska, P.-E. Milhiet, M. Zinke-Allmang, C. Le Grimellec, Phase topology and growth of single domains in lipid bilayers, Langmuir 17 (2001) 1653–1659.

[14] I. Reviakine, A. Brisson, Formation of supported phospholipid bilayers from unilamellar vesicles investigated by atomic force microscopy, Langmuir 16 (2000) 1806–1815.

[15] T. Kaasgaard, C. Leidy, J.H. Crowe, O.G. Mouritsen, K. Jorgensen, Temperature-controlled structure and kinetics of ripple phases in one- and two-component supported lipid bilayers, Biophys. J. 85 (2003) 350–360.

[16] V. Vie, N. Van Mau, E. Lesniewska, J.P. Goudonnet, F. Heitz, C. Le Grimellec, Distribution of ganglioside GM1 between two-component, two-phase phosphatidylcholine monolayers, Langmuir 14 (1998) 4574–4583.

[17] S. Morandat, K. El Kirat, Membrane resistance to Triton X-100 explored by real-time atomic force microscopy, Langmuir 22 (2006) 5786–5791.

[18] K. El Kirat, A. Pardo-Jacques, S. Morandat, Interaction of non-ionic detergents with biomembranes at the nanoscale observed by atomic force microscopy, Int. J. Nanotech (in press).

[19] S. Morandat, K. El Kirat, Solubilization of supported lipid membranes by octyl glucoside observed by time-lapse atomic force microscopy, Coll. Surf. B 55 (2007) 179–184.

[20] K. El Kirat, S. Morandat, Cholesterol modulation of membrane resistance to Triton X-100 explored by atomic force microscopy, Biochim. Biophys. Acta 1768 (2007) 2300–2309.

[21] H.A. Rinia, B. de Kruijff, Imaging domains in model membranes with atomic force microscopy, FEBS Lett. 504 (2001) 194–199.

[22] J. Mou, J. Yang, C. Huang, Z. Shao, Alcohol induces interdigitated domains in unilamellar phosphatidylcholine bilayers, Biochemistry 33 (1994) 9981–9985.

[23] J. Mou, J. Yang, Z. Shao, Tris(hydroxymethyl)aminomethane ($C_4H_{11}NO_3$) induced a ripple phase in supported unilamellar phospholipid bilayers, Biochemistry 33 (1994) 4439–4443.

[24] H.A. Rinia, J.W. Boots, D.T. Rijkers, R.A. Kik, M.M. Snel, R.A. Demel, J.A. Killian, J.P. van der Eerden, B. de Kruijff, Domain formation in phosphatidylcholine bilayers containing transmembrane peptides: specific effects of flanking residues, Biochemistry 41 (2002) 2814–2824.

[25] K. El Kirat, L. Lins, R. Brasseur, Y.F. Dufrene, Fusogenic tilted peptides induce nanoscale holes in supported phosphatidylcholine bilayers, Langmuir 21 (2005) 3116–3121.

[26] K. El Kirat, Y.F. Dufrene, L. Lins, R. Brasseur, The SIV tilted peptide induces cylindrical reverse micelles in supported lipid bilayers, Biochemistry 45 (2006) 9336–9341.

[27] P.E. Milhiet, M.C. Giocondi, O. Baghdadi, F. Ronzon, B. Roux, C. Le Grimellec, Spontaneous insertion and partitioning of alkaline phosphatase into model lipid rafts, EMBO Rep. 3 (2002) 485–490.

[28] M. Grandbois, H. Clausen-Schaumann, H. Gaub, Atomic force microscope imaging of phospholipid bilayer degradation by phospholipase A2, Biophys. J. 74 (1998) 2398–2404.

[29] L.K. Nielsen, J. Risbo, T.H. Callisen, T. Bjornholm, Lag-burst kinetics in phospholipase A(2) hydrolysis of DPPC bilayers visualized by atomic force microscopy, Biochim. Biophys. Acta 1420 (1999) 266–271.

[30] T. Kaasgaard, J.H. Ipsen, O.G. Mouritsen, K. Jorgensen, In situ phospholipase A2 degradation of one- and two-component phospholipid bilayers imaged by atomic force microscopy, Probe Microsc. 2 (2001) 169–175.

[31] H. Clausen-Schaumann, M. Grandbois, H.E. Gaub, Enzyme-assisted nanoscale lithography in lipid membranes, Adv. Mater. 10 (1998) 949–952.

[32] K. El Kirat, L. Lins, R. Brasseur, Y.F. Dufrene, Nanoscale modification of supported lipid membranes: synergistic effect of Phospholipase D and viral fusion peptide, J. Biomed. Nanotech. 1 (2005) 39–46.

[33] D. Geng, D.P. Baker, S.F. Foley, C. Zhou, K. Stieglitz, M.F. Roberts, A 20-kDa domain is required for phosphatidic acid-induced allosteric activation of Phospholipase D from *Streptomyces cromofuscus*, Biochim. Biophys. Acta 1430 (1999) 234–244.

[34] H.A. Rinia, R.A. Kik, R.A. Demel, M.M. Snel, J.A. Killian, J.P. Der Eerden, B. de Kruijff, Visualization of highly ordered striated domains induced by transmembrane peptides in supported phosphatidylcholine bilayers, Biochemistry 39 (2000) 5852–5858.

[35] J. Mou, D.M. Czajkowsky, Z. Shao, Gramicidin A aggregation in supported gel state phosphatidylcholine bilayers, Biochemistry 35 (1996) 3222–3226.

[36] P. Garidel, A. Blume, Calcium induced nonideal mixing in liquid-crystalline phosphatidylcholine-phosphatidic acid bilayer membranes, Langmuir 16 (2000) 1662–1667.

[37] J.J. Blum, J.A. Lehman, J.M. Horn, J. Gomez-Cambronero, Phospholipase D (PLD) is present in *Leishmania donovani* and its activity increases in response to acute osmotic stress, J. Eukaryot. Microbiol. 48 (2001) 102–110.

[38] H.A. Rinia, R.A. Demel, J.P. van der Eerden, B. de Kruijff, Blistering of Langmuir–Blodgett bilayers containing anionic phospholipids as observed by atomic force microscopy, Biophys. J. 77 (1999) 1683–1693.

[39] M. Liscovitch, Phospholipase D: role in signal transduction and membrane traffic, J. Lipid Mediators Cell Signal. 14 (1996) 215–221.

[40] T. Kobayashi, F. Gu, J. Gruenberg, Lipids, lipid domains and lipid-protein interactions in endocytic membrane traffic, Semin. Cell Dev. Biol. 9 (1998) 517–526.

[41] D. Jones, C. Morgan, S. Cockcroft, Phospholipase D and membrane traffic. Potential roles in regulated exocytosis, membrane delivery and vesicle budding, Biochim. Biophys. Acta 1439 (1999) 229–244.